

# DVCS via color dipoles: Nonperturbative effects

B.Z. Kopeliovich,<sup>\*</sup> Ivan Schmidt,<sup>†</sup> and M. Siddikov<sup>‡</sup>

*Departamento de Física y Centro de Estudios Subatómicos,  
Universidad Técnica Federico Santa María, Casilla 110-V, Avda. España 1680, Valparaíso, Chile*  
(Dated: December 19, 2008)

We study the DVCS amplitude within the color dipole approach. The light-cone wave function of a real photon is evaluated in the instanton vacuum model. Our parameter free calculations are able to describe H1 data, both the absolute values and the  $t$ -dependences, at medium-high values of  $Q^2$ . The  $Q^2$  dependence is found to be sensitive to the choice of the phenomenological cross section fitted to DIS data.

## I. INTRODUCTION

During the last decade hard exclusive reactions, such as deeply virtual compton scattering (DVCS),  $\gamma^* + p \rightarrow \gamma + p$ , have been a subject of intensive theoretical and experimental investigation [1, 2, 3, 4, 5, 6, 7, 8, 9, 10, 11, 12, 13, 14, 15]. Particular interest deserves the Bjorken kinematics,

$$-q^2 \equiv W^2 Q^2 \gg \Lambda_{QCD}^2, \quad W^2 \equiv (p+q)^2 \gg \Lambda_{QCD}^2, \quad (1)$$

$$x_B \equiv \frac{Q^2}{2P \cdot q} = const, \quad t \equiv \Delta^2 = (p' - p)^2 \ll Q^2, \quad (2)$$

where  $q$  is the momentum of the virtual photon,  $p$  is the momentum of the initial hadron,  $p'$  is the momentum of the final hadron, and  $t$  is the momentum transfer. In this kinematics the DVCS amplitude is factorized [7, 8] into the convolution of a perturbative coefficient function with a soft matrix element—generalized parton distribution (GPD) of the parton inside the target.

While for the region  $x \sim 1$  the dominant contribution to the DVCS amplitude comes from the generalized parton distributions (GPD) for quarks, we know from experience with deep-inelastic scattering (DIS) that in the small- $x$  kinematics (large c.m. energy  $W$ ) the density of partons (especially gluons) increases and the dominant contribution comes from the gluon sector.

In this paper we employ the color dipole approach introduced in [16, 17]. The central object of the model is the dipole scattering amplitude,  $\mathcal{A}(x, \vec{r})$ . For DIS, only the imaginary part of the amplitude contributes, and the result becomes especially simple [16, 18],

$$\sigma_{\gamma^* p}(x, Q^2) = \int_0^1 dz \int d^2r |\Psi(z, r, Q^2)|^2 \sigma_{\bar{q}q}(x, r), \quad (3)$$

—the DIS cross-section equals the dipole cross-section  $\sigma_{\bar{q}q}(x, r)$  “averaged” with weight  $|\Psi(z, r, Q^2)|^2$ , where  $\Psi(z, r, Q^2)$  is the virtual photon light-cone wave function, which depends on transverse separation  $\vec{r}$  and fraction  $z$  of the light-cone momentum carried by the quark (see Section III for rigorous definition).

Generalization of (3) to the DVCS case is straightforward [19, 20], although one has to pay attention to some subtle points. First, one has to deal with the nonperturbative contribution of large-size dipoles. While it also exists in the forward case (DIS), the problem is exacerbated in the off-forward case (DVCS) due to presence of the real photon in the final state. *A priori*, one cannot say how important this contribution is in a particular process. As a first approximation, one can just ignore the nonperturbative effects, as was done in [19, 20, 21, 22], and evaluate everything perturbatively. While for DIS this approximation is partially justified due to high virtualities  $Q^2$  in both vertices, for DVCS its validity is questionable, since the final photon is real. In the present evaluations we rely on the instanton vacuum model for the photon wave function.

Another complication is that in contrast to DIS, the DVCS amplitude is sensitive to both the real and imaginary parts of the dipole amplitude. In this evaluations we restore the real part using the prescription proposed in [23] (see Section II for more details).

<sup>\*</sup>Electronic address: Boris.Kopeliovich@usm.cl

<sup>†</sup>Electronic address: Ivan.Schmidt@usm.cl

<sup>‡</sup>Electronic address: Marat.Siddikov@usm.cl

The paper is organized as follows. In Section II we review the color dipole model and present the parameters used in numerical evaluations. In Section III we evaluate the photon wave function within the instanton vacuum model. In Sections IV and V we present results for the DVCS cross-sections, compare with available data, and draw conclusions.

## II. COLOR DIPOLE MODEL

As was mentioned above, the color dipole model is valid only in the region of small- $x$ , where the dominant contribution to the DVCS amplitude comes from gluonic exchanges. The general expression for the DVCS amplitude in the color dipole model has the form,

$$\mathcal{A}_{\mu\nu}(x_B, t, Q^2) \propto \epsilon_\mu^{(i)} \epsilon_\nu^{(j)} \int d\beta_1 d\beta_2 d^2 r_1 d^2 r_2 \bar{\Psi}^{(i)}(\beta_2, \vec{r}_2, Q^2 = 0) \mathcal{A}_{ij}^d(\beta_1, \vec{r}_1; \beta_2, \vec{r}_2; Q^2, \Delta) \Psi^{(j)}(\beta_1, \vec{r}_1, Q^2), \quad (4)$$

where  $\beta_{1,2}$  are the light-cone fractional momenta of the quark, and  $\vec{r}_{1,2}$  are the transverse distances in the final and initial states respectively (in off-forward kinematics they are no longer equal),  $\Delta$  is the momentum transfer in DVCS,  $\mathcal{A}^d(\dots)$  is the scattering amplitude for the dipole state, and indices  $(i, j)$  refer to polarizations of initial and final photons. In general case the amplitude  $\mathcal{A}^d(\dots)$  is a nonperturbative object, with asymptotic behaviour for small  $r$  determined from the pQCD [16]:

$$\mathcal{A}^d(\dots) \sim r^2 \quad (5)$$

(up to slowly varying corrections  $\sim \ln(r)$ ).

In our approach we use a model [24, 25, 26] for the partial amplitude of the scattering of the color dipole on the nucleon, which has the form

$$\mathcal{A}_{ij}^d(\beta_1, \vec{r}_1; \beta_2, \vec{r}_2; Q^2, \Delta) \approx \delta(\beta_1 - \beta_2) \delta(\vec{r}_1 - \vec{r}_2) \int d^2 b e^{i\vec{\Delta}\vec{b}} \text{Im} f_{\bar{q}q}^N(\vec{r}_1, \vec{b}, \beta_1) \quad (6)$$

$$\begin{aligned} \text{Im} f_{\bar{q}q}^N(\vec{r}, \vec{b}, \beta) &= \frac{1}{12\pi} \int \frac{d^2 k d^2 \Delta}{\left(\vec{k} + \frac{\vec{\Delta}}{2}\right)^2 \left(\vec{k} - \frac{\vec{\Delta}}{2}\right)^2} \alpha_s \mathcal{F}\left(x, \vec{k}, \vec{\Delta}\right) e^{i\vec{b}\cdot\vec{\Delta}} \\ &\times \left( e^{-i\beta\vec{r}\cdot\left(\vec{k} - \frac{\vec{\Delta}}{2}\right)} - e^{i(1-\beta)\vec{r}\cdot\left(\vec{k} - \frac{\vec{\Delta}}{2}\right)} \right) \left( e^{i\beta\vec{r}\cdot\left(\vec{k} + \frac{\vec{\Delta}}{2}\right)} - e^{-i(1-\beta)\vec{r}\cdot\left(\vec{k} + \frac{\vec{\Delta}}{2}\right)} \right), \end{aligned} \quad (7)$$

where  $\vec{b}$  is impact parameter;  $\left(\vec{k} - \frac{\vec{\Delta}}{2}, \vec{k} + \frac{\vec{\Delta}}{2}\right)$  are the transverse momenta of the incoming and outgoing quarks;  $\mathcal{F}\left(x, \vec{k}, \vec{\Delta}\right)$  is the *unintegrated* GPD for gluons [48],

$$\begin{aligned} \frac{\mathcal{F}\left(x, \vec{k}, \vec{\Delta}\right)}{k^2} &\equiv H\left(x, \vec{k}, \vec{\Delta}\right) \\ &= \frac{1}{2} \int d^2 r e^{i\vec{k}\cdot\vec{r}} \int \frac{dz^-}{2\pi} e^{ix\bar{P}^+ z^-} \left\langle P' \left| \bar{\psi}\left(-\frac{z}{2}, -\frac{\vec{r}}{2}\right) \gamma_+ \mathcal{L}_\infty\left(-\frac{z}{2}, -\frac{\vec{r}}{2}; \frac{z}{2}, \frac{\vec{r}}{2}\right) \psi\left(\frac{z}{2}, \frac{\vec{r}}{2}\right) \right| P \right\rangle, \end{aligned} \quad (8)$$

where  $\mathcal{L}_\infty(x; y)$  is the Wilson factor required by gauge covariance. For this GPD we use the gaussian parameterization [24, 25, 26],

$$\mathcal{F}\left(x, \vec{k}, \vec{\Delta}\right) = \frac{3\sigma_0(x)}{16\pi^2\alpha_s} \left(\vec{k} + \frac{\vec{\Delta}}{2}\right)^2 \left(\vec{k} - \frac{\vec{\Delta}}{2}\right)^2 R_0^2(x) \exp\left(-\frac{R_0^2(x)}{4} \left(\vec{k}^2 + \frac{\vec{\Delta}^2}{4}\right)\right) \exp\left(-\frac{1}{2}B(x)\vec{\Delta}^2\right), \quad (9)$$

where  $\sigma_0(x)$ ,  $R_0^2(x)$ ,  $B(x)$  are free parameters fixed from the DIS and  $\pi p$  scattering data. We shall discuss them in more detail in Section IV. The parameterization (9) does not depend on the longitudinal momentum transfer and decreases exponentially as a function of  $\Delta^2$ . Since it is an effective parameterization valid only in the small- $x$  region, we do not assume that it satisfies general requirements, such as positivity [27] and polynomiality [3] constraints.

The prefactor  $\left(\vec{k} + \frac{\vec{\Delta}}{2}\right)^2 \left(\vec{k} - \frac{\vec{\Delta}}{2}\right)^2$  in (9) guarantees convergence of the integrals in equation (6). In the forward limit, the amplitude (6) reduces to the saturated parameterization of the dipole amplitude proposed by Golec-Biernat

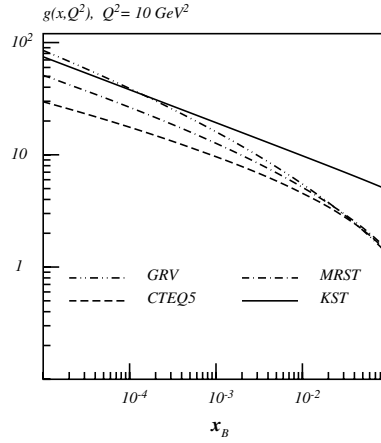


FIG. 1: Comparison of  $k$ -integrated forward limit  $g_{BK}(x, Q^2)$  of parameterization (9) with realistic parameterizations: GRV [29], MRST [30] and CTEQ5 [31].

and Wüsthoff (GBW) [28]. The corresponding  $k$ -integrated forward limit of the GPD (9) is compared with realistic parameterizations of the gluon PDFs - GRV [29], MRST [30] and CTEQ5 [31] in the Figure (1). We find that in the region  $x \lesssim 10^{-3}$  the parameterization (9) agrees, within experimental and theoretical uncertainties, with these realistic parameterizations, but deviates for larger  $x$ .

Taking the integrals in (6), we arrive at

$$\begin{aligned} \text{Im} f_{\bar{q}q}^N(\vec{r}, \vec{\Delta}, \beta) &= \int d^2b e^{i\vec{b}\vec{\Delta}} \text{Im} f_{\bar{q}q}^N(\vec{r}, \vec{b}, \beta) = \frac{\sigma_0(s)}{4} \exp\left(-\left(\frac{B(s)}{2} + \frac{R_0^2(s)}{16}\right) \vec{\Delta}_\perp^2\right) \times \\ &\times \left(e^{-i\beta\vec{r}\cdot\vec{\Delta}} + e^{i(1-\beta)\vec{r}\cdot\vec{\Delta}} - 2e^{i(\frac{1}{2}-\beta)\vec{r}\cdot\vec{\Delta}} e^{-\frac{\vec{r}^2}{R_0^2(x)}}\right). \end{aligned} \quad (10)$$

Evaluation of the real part of the amplitude is quite straightforward. As it was discussed in [23], if the limit  $\lim_{s \rightarrow \infty} \left(\frac{\text{Im} \mathcal{A}}{s^\alpha}\right)$  exists and is finite, then the real part of the amplitude is related with imaginary part by

$$\text{Re} \mathcal{A} = s^\alpha \tan\left[\frac{\pi}{2} \left(\alpha - 1 + \frac{\partial}{\partial \ln s}\right)\right] \frac{\text{Im} \mathcal{A}}{s^\alpha}. \quad (11)$$

As it will be shown in Section IV, the imaginary part in the color dipole model indeed has a power dependence on energy,  $\text{Im} \mathcal{A}(s) \sim s^\alpha$ . The formula (11) in this case may be simplified to

$$\frac{\text{Re} \mathcal{A}}{\text{Im} \mathcal{A}} = \tan\left(\frac{\pi}{2}(\alpha - 1)\right) := \eta. \quad (12)$$

Then for the DVCS amplitude we finally obtain

$$\mathcal{A}_{\mu\nu}^{(ij)} \approx (\eta + i)\epsilon_\mu^{(i)}(q')\epsilon_\nu^{(j)}(q) \int d^2r \int d\beta \bar{\Psi}^{(i)}(\beta, r, Q^2 = 0) \Psi^{(j)}(\beta, r, Q^2) \text{Im} f_{\bar{q}q}^N(\vec{r}, \vec{\Delta}, \beta), \quad (13)$$

where in (13) the upper indices  $(ij)$  refer to polarizations of the final and initial states, and we evaluated the real part of the DVCS amplitude according to (11). For the cross-section of unpolarised DVCS amplitude, from (13) we obtain[49]

$$\begin{aligned} \frac{d\sigma}{dt} &= \frac{1 + \eta^2}{16\pi} \sum_{ij} \left| \mathcal{A}_{\mu\nu}^{(ij)} \right|^2 = \\ &= \frac{1 + \eta^2}{16\pi} \sum_{ij} \left| \int d^2r \int d\beta \bar{\Psi}^{(i)}(\beta, r, Q^2 = 0) \Psi^{(j)}(\beta, r, Q^2) i \text{Im} f_{\bar{q}q}^N(\vec{r}, \vec{\Delta}, \beta) \right|^2. \end{aligned} \quad (14)$$

Since the helicity-flip scattering is a higher-twist effect, it is suppressed in the large- $Q^2$  kinematics. Thus we may further simplify (14) to

$$\frac{d\sigma}{dt} \approx \frac{1 + \eta^2}{16\pi} \sum_i \left| \int d^2r \int d\beta \bar{\Psi}^{(i)}(\beta, r, Q^2 = 0) \Psi^{(i)}(\beta, r, Q^2) i \text{Im} f_{\bar{q}q}^N(\vec{r}, \vec{\Delta}, \beta) \right|^2. \quad (15)$$

Formula (15) is the final result which will be used for numerical evaluation of the DVCS amplitude. It is important to note that in the small- $r$  region the amplitude (10) behaves as  $\mathcal{A} \sim r^2$ , therefore the corresponding cross-section (14) is falling as  $1/Q^4$  at large- $Q^2$ , in agreement with the general analysis [1, 2, 7].

### III. PHOTON WAVE FUNCTION IN THE INSTANTON VACUUM

In this section we would like to provide some details of evaluation of the wave function in the instanton vacuum model (IVM) (see [32, 33, 34, 35, 36] and references therein). In the leading order in  $N_c$ , the model has the same Feynman rules as in the perturbative theory, but with momentum-dependent quark mass  $\mu(p)$  in the quark propagator [33]

$$S(p) = \frac{1}{\hat{p} - \mu(p) + i0}, \quad (16)$$

and nonlocal interaction vertex of vector current [35]

$$\hat{v} \equiv v_\mu \gamma^\mu \rightarrow \hat{V} = \hat{v} - M (G_\mu(p, q) f(p+q) + G_\mu(p+q, -q) f(p)) v^\mu(q), \quad (17)$$

$$G_\mu(p, q) \equiv \sum_{n=0}^{\infty} \frac{1}{(n+1)!} f_{,\mu,\mu_1\dots\mu_n} q_{\mu_1}\dots q_{\mu_n} \approx f_{,\mu}(p) + \mathcal{O}(q), \quad (18)$$

where  $p, p+q$  are the momenta of the incoming and outgoing quarks respectively, and  $f_{,\mu_1\dots\mu_n}(p) \equiv \partial^n f(p)/\partial p_{\mu_1}\dots\partial p_{\mu_n}$ . Using symmetry properties of the the last term in (17) and properties of the function  $G_\mu(p, q)$ , it is possible to cast (17) to the equivalent form

$$\hat{V} = v^\mu(q) \left( \gamma_\mu - (2p_\mu + q_\mu) \frac{M (f^2(p+q) - f^2(p))}{(p+q)^2 - p^2} \right), \quad (19)$$

which is frequently used [37, 38].

The mass of the constituent quark has a form [33]

$$\mu(p) = m + M f^2(p), \quad (20)$$

where  $m \approx 5$  MeV is the current quark mass, and  $M \approx 350$  MeV is the contribution of the instanton-induced effects. In the limit  $p \rightarrow \infty$  the instanton-induced nonlinear formfactor  $f(p)$  falls off as  $\sim \frac{1}{p^3}$ , so for large  $p \gg \rho^{-1}$ , where  $\rho \approx (600 \text{ MeV})^{-1}$  is the average instanton size, the mass of the quark  $\mu(p) \approx m$  and the vector current interaction vertex  $\hat{V} \approx \hat{v}$ . However, we would like to emphasize that all the correlators get contributions from both the soft and the hard parts, so even in the large- $Q$  limit the instanton vacuum wave function is different from the well-known QED result.

The overlap of the initial and final photon wave functions in (15) was evaluated according to

$$\Psi^{(i)*}(\beta, r, Q^2 = 0) \Psi^{(i)}(\beta, r, Q^2) = \sum_{\Gamma} I_{\Gamma}^*(\beta, r^*, 0) I_{\Gamma}(\beta, r, Q^2), \quad (21)$$

where the summation is done over possible polarization states  $\Gamma_{em} = \{\gamma_\mu, \gamma_\mu \gamma_5, \sigma_{\mu\nu}\}$ , and  $I_{\Gamma}$  corresponds to one of the matrix elements

$$I_{\mu}(\beta, \vec{r}) = \int \frac{dz^-}{2\pi} e^{i(\beta+\frac{1}{2})q^-z^+} \left\langle 0 \left| \bar{\psi} \left( -\frac{z}{2}, -\frac{\vec{r}}{2} \right) \gamma_{\mu} \psi \left( \frac{z}{2}, \frac{\vec{r}}{2} \right) \right| \gamma(q) \right\rangle, \quad (22)$$

$$I_{\mu}^5(\beta, \vec{r}) = \int \frac{dz^-}{2\pi} e^{i(\beta+\frac{1}{2})q^-z^+} \left\langle 0 \left| \bar{\psi} \left( -\frac{z}{2}, -\frac{\vec{r}}{2} \right) \gamma_{\mu} \gamma_5 \psi \left( \frac{z}{2}, \frac{\vec{r}}{2} \right) \right| \gamma(q) \right\rangle, \quad (23)$$

$$I_{\mu\nu}(\beta, \vec{r}) = \int \frac{dz^-}{2\pi} e^{i(\beta+\frac{1}{2})q^-z^+} \left\langle 0 \left| \bar{\psi} \left( -\frac{z}{2}, -\frac{\vec{r}}{2} \right) \sigma_{\mu\nu} \psi \left( \frac{z}{2}, \frac{\vec{r}}{2} \right) \right| \gamma(q) \right\rangle. \quad (24)$$

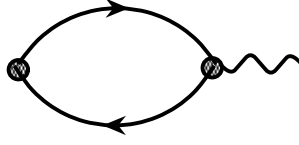


FIG. 2: In the leading order there is only one diagram which contributes to the wave function (25).

Notice also that in the final state in 21 we should use  $r_\mu^* = r_\mu + n_\mu \frac{q'_\perp \cdot r_\perp}{q_+} = r_\mu - n_\mu \frac{\Delta_\perp \cdot r_\perp}{q_+}$ , which takes into account that the final photon has  $q'_\perp \neq 0$  whereas the components of the wave function (22-24) are defined in the reference frame with  $q_\perp = 0$ .

The wave functions corresponding to matrix elements (22-24) were evaluated in [36]. In the leading order in  $N_c$  one can easily obtain for the components  $I_\Gamma$

$$I_\Gamma = \int \frac{d^4 p}{(2\pi)^4} e^{i\vec{p}_\perp \cdot \vec{r}_\perp} \delta \left( p^+ - \left( \beta + \frac{1}{2} \right) q^+ \right) \text{Tr} \left( S(p) \hat{V} S(p+q) \Gamma_{em} \right), \quad (25)$$

which corresponds to the diagram shown in the Figure (2). The evaluation of (25) is quite straightforward and in the reference frame with  $q_\perp = 0$ ,  $\epsilon_\lambda^{(i)}(q) = \epsilon_{\lambda_\perp}^{(i)}(q)$  yields

$$I_\mu(\beta, r) = \int dz^- e^{-i(\beta-1/2)q^+ z^-} \left\langle 0 \left| \bar{\psi} \left( -\frac{z}{2}, -\frac{\vec{r}}{2} \right) \gamma_\mu \psi \left( \frac{z}{2}, \frac{\vec{r}}{2} \right) \right| \gamma^\lambda(q) \right\rangle \quad (26)$$

$$= -ie_q \epsilon_\nu^{(\lambda)}(q) \int \frac{d^3 p}{(2\pi)^3} e^{-ir_\perp \cdot (p + \frac{q}{2})} \times$$

$$\times \left( \frac{p_\mu(p+q)^\nu + p^\nu(p+q)_\mu - (p^2 + p \cdot q - \mu(p)\mu(p+q)) \delta_\mu^\nu}{(2\beta q^+ p^- - p_\perp^2 - \mu^2(p) + i0) \left( 2(1-\beta)q^+ \left( p^- - \frac{Q^2}{2q^+} \right) - p_\perp^2 - \mu^2(p+q) + i0 \right)} \right.$$

$$\left. - \frac{M(G_\nu(p, q) f(p+q) + f(p) G_\nu(p+q, -q)) (\mu(p)(p+q)_\mu + \mu(p+q)p_\mu)}{(2\beta q^+ p^- - p_\perp^2 - \mu^2(p) + i0) \left( 2(1-\beta)q^+ \left( p^- - \frac{Q^2}{2q^+} \right) - p_\perp^2 - \mu^2(p+q) + i0 \right)} \right),$$

$$I_\mu^5(\beta, r) = \int dz^- e^{-i(\beta-1/2)q^+ z^-} \left\langle 0 \left| \bar{\psi} \left( -\frac{z}{2}, -\frac{\vec{r}}{2} \right) \gamma_\mu \gamma_5 \psi \left( \frac{z}{2}, \frac{\vec{r}}{2} \right) \right| \gamma^\lambda(q) \right\rangle \quad (27)$$

$$= -ie_q \epsilon_{\mu\alpha\beta\gamma} \epsilon^{\alpha(\lambda)}(q) q^\beta 4N_c \int \frac{d^3 p}{(2\pi)^3} e^{-ir_\perp \cdot (p + \frac{q}{2})} \times$$

$$\times \frac{p_\gamma}{(2\beta q_+ p_- - p_\perp^2 - \mu^2(p) + i0) \left( 2(1-\beta)q_+ \left( p_- - \frac{Q^2}{2q_+} \right) - p_\perp^2 - \mu^2(p+q) + i0 \right)}$$

$$I_{\mu\nu}(\beta, r) = \int dz_- e^{-i(\beta-1/2)q_+ z_-} \left\langle 0 \left| \bar{\psi} \left( -\frac{z}{2}, -\frac{\vec{r}}{2} \right) \sigma_{\mu\nu} \psi \left( \frac{z}{2}, \frac{\vec{r}}{2} \right) \right| \gamma^\lambda(q) \right\rangle \quad (28)$$

$$= -ie_q \epsilon_\lambda^{(i)}(q) \int \frac{d^3 p}{(2\pi)^3} e^{-ir_\perp \cdot (p + \frac{q}{2})} \times$$

$$\times \frac{\mu(p)(q_\nu g_{\mu\lambda} - q_\mu g_{\nu\lambda}) + (\mu(p+q) - \mu(p))(p_\mu g_{\nu\lambda} - p_\nu g_{\mu\lambda}) + M(G_\lambda(p, q) f(p+q) + f(p) G_\lambda(p+q, -q))(p_\mu q_\nu - p_\nu q_\mu)}{(2\beta q^+ p^- - p_\perp^2 - \mu^2(p) + i0) \left( 2(1-\beta)q^+ \left( p^- - \frac{Q^2}{2q^+} \right) - p_\perp^2 - \mu^2(p+q) + i0 \right)}$$

We evaluated (26-28) numerically.

#### IV. RESULTS

Here we present the results of the evaluation of the DVCS differential cross section with different models for the partial dipole amplitude  $f_{q\bar{q}}^N(\vec{r}, \vec{b})$ , and we also use a photon wave function calculated either perturbatively, or within the instanton vacuum model. First we test the amplitude based on the GBW model. We also perform calculations with the parameterization proposed by Kowalski and Teaney (KT) for the saturated dipole cross section [39]. In addition, we try an energy dependent KST parameterization for the dipole cross section, proposed in [25, 26, 40].

### A. GBW based partial dipole amplitude

First of all, we made evaluations in the GBW model [28] extended to the  $b$ -dependent partial amplitude  $f_{\bar{q}q}^N(\vec{r}, \vec{b})$ . This parameterization is fitted to DIS data at large  $Q^2$  and small Bjorken  $x$ . The parameters in Eq. (9) read,  $\sigma_0(x) = 23.03 \text{ mb} = \text{const}$ ,  $R_0(x) = 0.4 \times (x/x_0)^{0.144} \text{ fm}$ , where  $x_0 = 3.04 \times 10^{-4}$ . The parameter  $B(x)$  in Eq. (9), is related to the  $t$ -slope of the differential cross section of highly virtual photoproduction of vector mesons [24, 25, 26],

$$B(x) = B_{\gamma^* p \rightarrow \rho p} - \frac{1}{8} R_0^2(x) \quad (29)$$

We use the experimental value of the slope  $B_{\gamma^* p \rightarrow \rho p}(x, Q^2 \gg 1 \text{ GeV}^2) \approx 5 \text{ GeV}^{-2}$  [41].

Following [28], we use the perturbative wave function of the photon with constituent quark mass 140 MeV. From the left panel of Figure 3 we see that in the small- $x_B$  region the cross-section is proportional to a power of  $x_B$ ,  $d\sigma/dt \sim x_B^\alpha$ , where the power  $\alpha$  was obtained by fitting the  $x_B$ -dependence in the range  $x_B \in (10^{-5}, 10^{-3})$  and slowly depends on  $(Q^2, t)$ .

In the right panel of Figure 3 we compare the model with data from the H1 experiment at HERA [42]. Although the model gives a reasonable description of the data at moderate values of  $Q^2$ , the discrepancy increases at higher  $Q^2$ . As it was discussed in Section II, the modeled DVCS cross-section falls as  $1/Q^4$ , while the data behave approximately as  $1/Q^3$ .

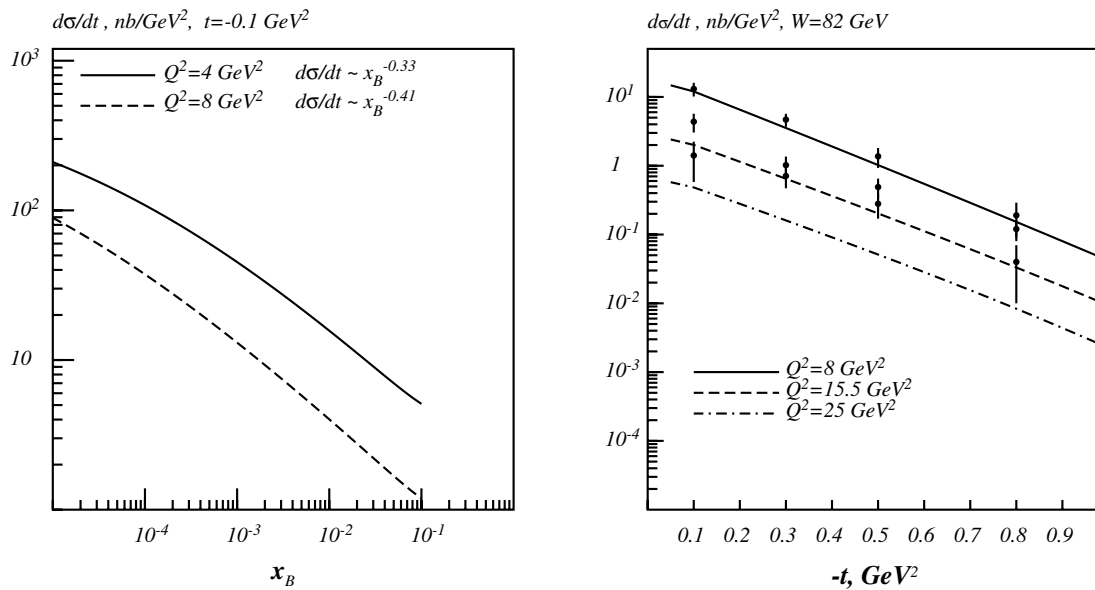


FIG. 3:  $x_B$ - and  $t$ -dependence of the DVCS cross-section in GBW parameterization

In order to identify the source of the disagreement, we replace the perturbative photon wave function by the one calculated in Section III within the model of instanton vacuum. The results are depicted in Figure 4. We see that the cross sections do not change very much compared to the previous calculation. This model gives a reasonable description of the cross-section for moderate  $Q^2$ , however grossly underestimates the data at high  $Q^2$ .

While the GBW dipole cross section does a pretty good job describing DIS data, and electroproduction of vector mesons [43, 44], it fails to explain the observed  $Q^2$  dependence in DVCS. This fact shows that DVCS provides a rather sensitive test for models.

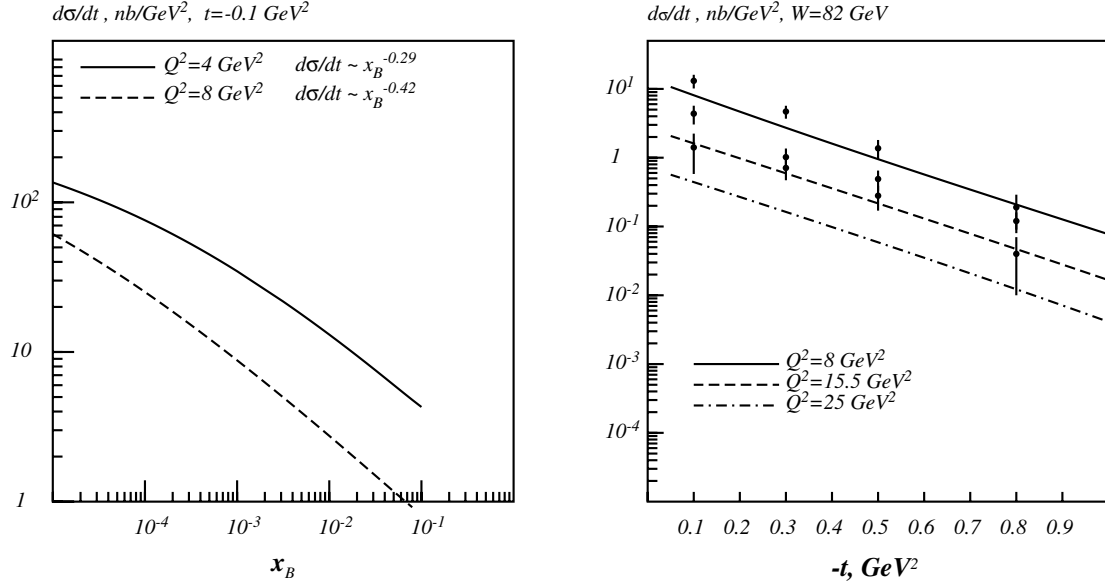


FIG. 4:  $x_B$ - and  $t$ -dependence of the DVCS cross-section in GBW parameterization, with realistic photon wave function.

### B. KT parameterization

Another form of impact parameter dependent partial dipole amplitude, which has correct behavior at small  $r$  and the saturated shape, was proposed in [39],

$$\text{Im}f(\vec{r}, \vec{b}) = 2 \left( 1 - \exp \left( -\frac{\pi^2}{6} r^2 \alpha_s(\mu^2) x g(x, \mu^2) T_N(b) \right) \right), \quad (30)$$

where the scale  $\mu^2 = 0.77 \text{ GeV}^2 + 4/r^2$ ; and the gluon distribution function  $g(x, \mu^2)$  was fitted to DIS data. The nucleon profile function in [39],  $T_N(b)$ , has a simple form

$$T_N(b) = \frac{1}{2\pi B_g} e^{-b^2/2B_g}, \quad (31)$$

where the slope parameters  $B_g = 4 \text{ GeV}^{-2}$  was fitted to data on electroproduction of vector mesons.

In the small- $r^2$  limit this function corresponds to ordinary gluon PDF  $g(x, \mu^2)$ . However, the latter may be different from the results of DGLAP analyses of data, since Eq. (30) is supposed to include the saturation effects. On the other hand, the eikonalization used in (30) is quite a rough procedure at large  $r$  where saturation is at work. A more accurate formula should include a convolution of the dipole amplitude with  $T_N(b)$ , rather than the simple product. This is why Eq. (30) misses correlations between  $\vec{b}$  and  $\vec{r}$ , which are present in (7).

Results for the DVCS differential cross section, calculated with this parameterization and the realistic nonperturbative photon wave function, are presented in Figure 5.

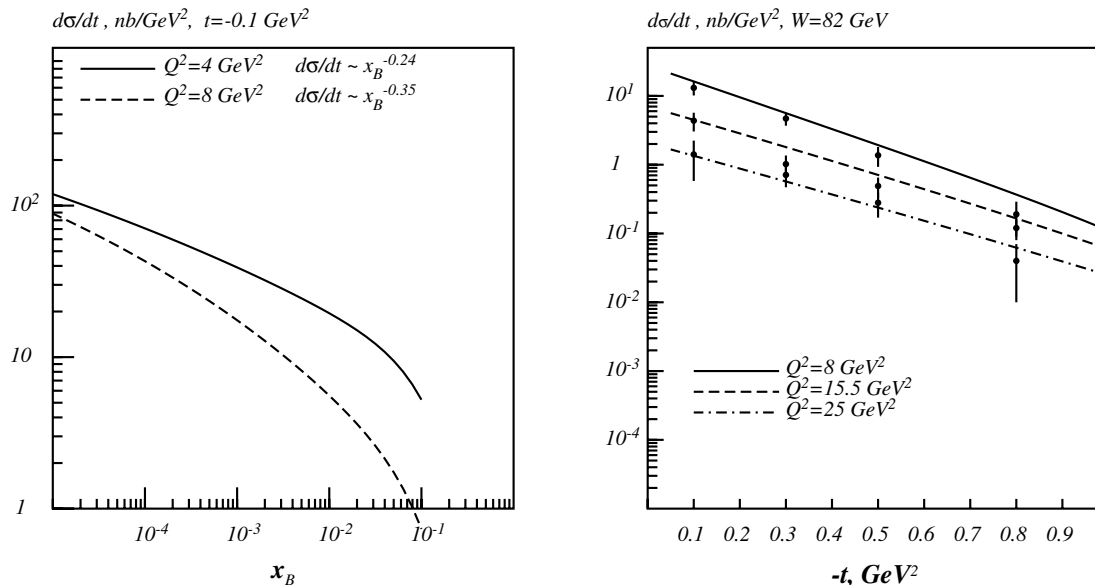


FIG. 5:  $x_B$ - and  $t$ -dependence of the DVCS cross-section in KT parameterization [39] with the realistic photon wave function.

### C. Energy dependent (KST) parameterization

While in the large- $Q^2$  kinematics scaling implies that the dipole amplitude is a function of Bjorken  $x$ , for smaller  $Q^2$  (soft photons) scaling does not work, and for real photons Bjorken  $x$  is not an appropriate variable. For this kinematics the photon energy  $s$  should be used instead of  $x_B$ . An  $s$ -dependent parameterization with saturated form analogous to the GBW was proposed in [45], for the description of the real photo production and absorption, and for DIS at small  $Q^2$ . One should replace all the  $x$ -dependent functions in Eq. (9) by  $s$ -dependent ones, with

$$\sigma_0(s) = \sigma_{tot}^{\pi p}(s) \left( 1 + \frac{3 R_0^2(s)}{8 \langle r_{ch}^2 \rangle} \right), \quad (32)$$

where  $\sigma_{tot}^{\pi p}(s) = (\Sigma_0 + \Sigma_1 \ln^2(s/s_0))$  with  $\Sigma_0 = 20.9 mb$ ,  $\Sigma_1 = 0.31 mb$ , and  $s_0 = 28.9 GeV^2$ , is the total pion-proton cross section, and  $\langle r_{ch}^2 \rangle \approx 0.44 fm^2$  is the pion charge radius. Correspondingly,  $R_0(s) = 0.88(s/s_1)^{0.14} fm$ ;  $s_1 = 1000 GeV^2$ . In this case the parameter  $B(s)$  is related to the  $t$ -slope of elastic  $\pi p$  scattering [25, 26],

$$B(s) = B_{el}^{\pi p}(s) - \frac{1}{8} R_0^2(s) - \frac{1}{3} \langle r_{ch}^2 \rangle. \quad (33)$$

Naturally, we use the nonperturbative photon wave function Eq. (21).

The numerical results for the DVCS cross section are depicted in Figure 6. Comparison with data plotted in the right panel show that this model also leads to a too steep  $Q^2$  dependence of the cross section, although its absolute value at  $Q^2 = 8 GeV^2$  agrees with the data.



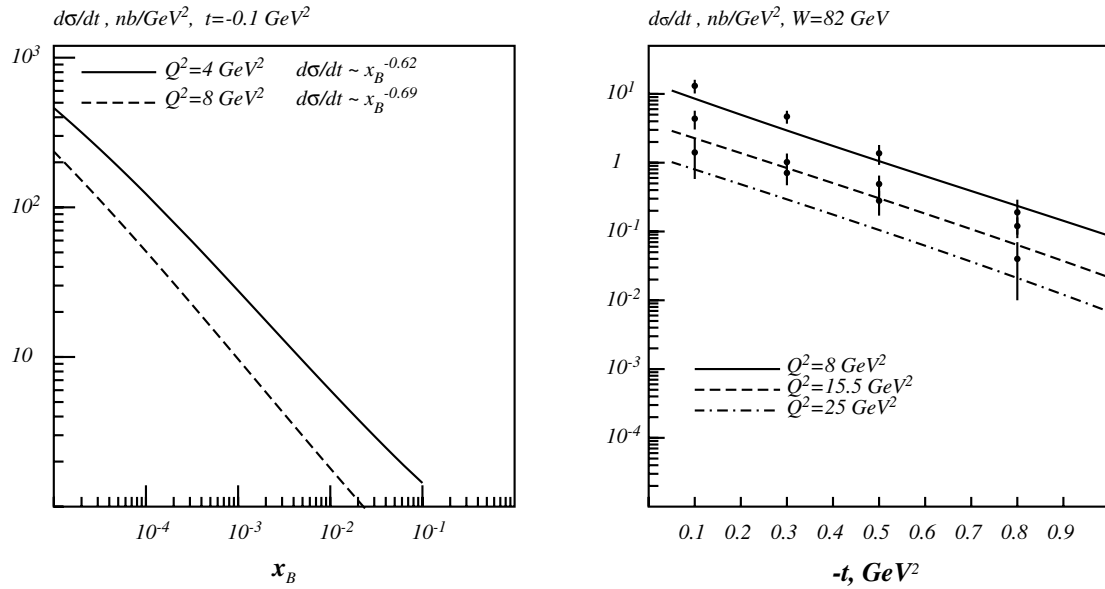


FIG. 6:  $x_B$ - and  $t$ -dependence of the DVCS cross-section, in KST parameterization, with realistic photon wave function.

## V. DISCUSSION AND CONCLUSIONS

In this paper we evaluated the DVCS cross-section relying on a nonperturbative wave function of the real photon calculated in the instanton vacuum model. The ratio of DVCS cross sections calculated with the IVM and perturbative wave functions is shown in the left panel of Figure 7 as function of  $t$  for different values of  $Q^2$ .

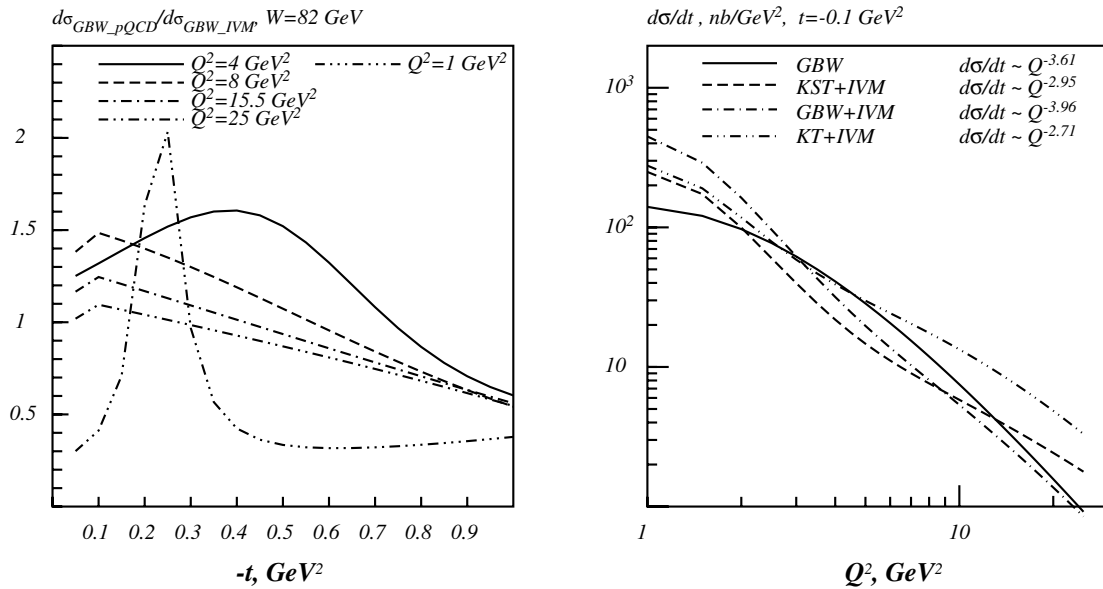


FIG. 7: Left: Ratio of the DVCS cross-section with pQCD and IVM wave functions in GBW model. One can clearly see that for  $Q^2 \sim 8 \text{ GeV}^2$  the difference might reach up to 50% (GBW and KST).

This comparison demonstrates a considerable modification of the cross section up to factor two, dependent on kinematics. For small- $Q^2 \sim 1 \text{ GeV}^2$  one should use instanton wave functions both for the initial and final photons. Note that even for  $Q^2 \sim 1 \text{ GeV}^2$  both cross-sections  $d\sigma_{IVM}/dt$  and  $d\sigma_{pQCD}/dt$  decrease quite fast as a function of  $t$ , approximately as  $e^{Bt}$ , as one can see from the previous Figures 3-5. The difference is due to the higher-twist effects which are amplified in the small- $Q^2$  region and become pronounced in the ratio of the cross-sections.

We also tested several models for the dipole cross section. Although all the parameterizations under discussion have been fitted to DIS data from HERA, not all of them are successful in describing the DVCS cross section, especially the observed  $Q^2$  dependence. In particular the dipole partial amplitude based on the popular GBW parameterization of the total cross section leads to a too steep  $Q^2$  dependence of the DVCS cross section, calculated with both IVM and perturbative photon wave functions. In this model the cross-section decreases in the measured interval  $Q^2 = 8 - 25 \text{ GeV}^2$  as  $1/Q^4$ , like one should expect at very large  $Q^2$  in accordance with the general large- $Q^2$  analysis [1, 2, 7], whereas H1 data exhibit an approximate  $\sim 1/Q^3$ -behaviour. We compare the  $Q^2$ -dependences calculated with different models for the photon wave function and dipole partial amplitude, at fixed  $x_B$  and  $t$  in the right panel of Figure 7. We also show in the Figure the results of the fit to the calculated cross sections within the  $Q^2$  interval measured in the H1 experiment. We conclude that although the absolute value of the cross-section is sensitive to the nonperturbative effects (large-size dipoles), the  $Q^2$ -dependence does not vary much.

Apparently, one can achieve a weaker  $Q^2$  dependence by replacing the standard quadratic  $r^2$  behavior of the dipole cross section predicted by pQCD at small  $r$  [16] by a smaller power of  $r$ . Such a model [46] was considered in [22] to describe the  $Q^2$ -dependence of H1 data for DVCS cross section by modifying the small- $r$  behaviour to  $\mathcal{A}_d \sim r^{1.35 + \text{const} \ln r}$ . This explains why the model gives reasonable description for the  $Q^2$ -dependence of the cross-section.

Remarkably, the KT model [47], considered above in section IV B provides a reasonable description of the measured  $Q^2$ , although it has the same small- $r$  behaviour  $\mathcal{A}_d \sim r^2$  as GBW. This happens because the higher-twist effects in this model are more pronounced than in GBW. Straightforward expansion of the dipole amplitude  $\mathcal{A}_d$  in the KT parameterization yields (we consider the case  $\Delta_\perp = 0$  for the sake of simplicity),

$$\mathcal{A}_d \sim r^2 [1 - \lambda_{KT}(r) r^2 + \mathcal{O}(r^4)], \quad (34)$$

where the constant  $\lambda_{KT}(r)$  depends on  $r$  only logarithmically, and for typical  $\langle r \rangle \sim \langle Q \rangle^{-1} \sim 0.1 \text{ GeV}^{-1}$  we have  $\lambda_{KT}(r) \sim 0.159 \text{ GeV}^2$ , which is larger than in GBW.

We would like to emphasize that although it is possible to fit the DIS data with a parameterization containing sufficient number of free parameters, not all of the available parameterizations are able to describe the DVCS data, and a systematic study of the higher-twist corrections is necessary. In this paper we addressed one of the possible sources-the higher-twist corrections to the wave function of the initial photon and considered realistic wave function for the final (real) photon. Other sources of higher-twist corrections include contributions of higher-twist quark-gluon operators, such as  $\langle p' | \bar{q}q | p \rangle$ ,  $\langle p' | \bar{q}G_+^\alpha G_{+\alpha}q | p \rangle$  etc. Contrary to DIS and heavy meson electroproduction, in most of other processes the large- $r$  behaviour of the amplitude *is* important and gives contribution comparable to the small- $r$  region. That's why in modelling of the large- $r$  behaviour of the amplitude we should refer to some microscopic model rather than to a semiphenomenological approach.

### Acknowledgments

We would like to thank A. Dorokhov and M. Musakhanov for discussion of the wave function in the instanton vacuum. This work was supported in part by Fondecyt (Chile) grant 1050589, and by DFG (Germany) grant PI182/3-1.

- 
- [1] D. Mueller, D. Robaschik, B. Geyer, F. M. Dittes and J. Horejsi, Fortsch. Phys. **42**, 101 (1994) [arXiv:hep-ph/9812448].
  - [2] X. D. Ji, Phys. Rev. D **55**, 7114 (1997).
  - [3] X. D. Ji, J. Phys. G **24**, 1181 (1998) [arXiv:hep-ph/9807358].
  - [4] A. V. Radyushkin, Phys. Lett. B **380**, 417 (1996) [arXiv:hep-ph/9604317].
  - [5] A. V. Radyushkin, Phys. Rev. D **56**, 5524 (1997).
  - [6] A. V. Radyushkin, arXiv:hep-ph/0101225.
  - [7] X. D. Ji and J. Osborne, Phys. Rev. D **58** (1998) 094018 [arXiv:hep-ph/9801260].
  - [8] J. C. Collins and A. Freund, Phys. Rev. D **59**, 074009 (1999).
  - [9] J. C. Collins, L. Frankfurt and M. Strikman, Phys. Rev. D **56**, 2982 (1997).
  - [10] S. J. Brodsky, L. Frankfurt, J. F. Gunion, A. H. Mueller and M. Strikman, Phys. Rev. D **50**, 3134 (1994).
  - [11] K. Goeke, M. V. Polyakov and M. Vanderhaeghen, Prog. Part. Nucl. Phys. **47**, 401 (2001) [arXiv:hep-ph/0106012].
  - [12] M. Diehl, T. Feldmann, R. Jakob and P. Kroll, Nucl. Phys. B **596**, 33 (2001) [Erratum-ibid. B **605**, 647 (2001)] [arXiv:hep-ph/0009255].
  - [13] A. V. Belitsky, D. Mueller and A. Kirchner, Nucl. Phys. B **629**, 323 (2002) [arXiv:hep-ph/0112108].
  - [14] M. Diehl, Phys. Rept. **388**, 41 (2003) [arXiv:hep-ph/0307382].

- [15] A. V. Belitsky and A. V. Radyushkin, Phys. Rept. **418**, 1 (2005) [arXiv:hep-ph/0504030].
- [16] B. Z. Kopeliovich, L. I. Lapidus and A. B. Zamolodchikov, JETP Lett. **33** (1981) 595 [Pisma Zh. Eksp. Teor. Fiz. **33** (1981) 612].
- [17] A. H. Mueller, Nucl. Phys. B **335**, 115 (1990); A. H. Mueller and B. Patel, Nucl. Phys. B **425**, 471 (1994) [arXiv:hep-ph/9403256].
- [18] N. N. Nikolaev and B. G. Zakharov, Phys. Lett. B **327** (1994) 149 [arXiv:hep-ph/9402209].
- [19] M. McDermott, R. Sandapen and G. Shaw, Eur. Phys. J. C **22**, 655 (2002) [arXiv:hep-ph/0107224].
- [20] L. Favart and M. V. T. Machado, Eur. Phys. J. C **29**, 365 (2003) [arXiv:hep-ph/0302079].
- [21] M. V. T. Machado, Braz. J. Phys. **37** (2007) 555.
- [22] M. V. T. Machado, arXiv:0810.3665 [hep-ph].
- [23] J. B. Bronzan, G. L. Kane and U. P. Sukhatme, Phys. Lett. B **49** (1974) 272.
- [24] B. Z. Kopeliovich, H. J. Pirner, A. H. Rezaeian and I. Schmidt, Phys. Rev. D **77** (2008) 034011 [arXiv:0711.3010 [hep-ph]].
- [25] B. Z. Kopeliovich, A. H. Rezaeian and I. Schmidt, arXiv:0809.4327 [hep-ph], to appear in Phys. Rev. D.
- [26] B. Z. Kopeliovich, I. K. Potashnikova, I. Schmidt and J. Soffer, arXiv:0805.4534 [hep-ph].
- [27] P. V. Pobylitsa, Phys. Rev. D **65** (2002) 114015 [arXiv:hep-ph/0201030].
- [28] K. J. Golec-Biernat and M. Wüsthoff, Phys. Rev. D **59** (1999) 014017 [arXiv:hep-ph/9807513].
- [29] M. Gluck, P. Jimenez-Delgado and E. Reya, Eur. Phys. J. C **53** (2008) 355 [arXiv:0709.0614 [hep-ph]].
- [30] A. D. Martin, W. J. Stirling and R. S. Thorne, Phys. Lett. B **636** (2006) 259 [arXiv:hep-ph/0603143].
- [31] H. L. Lai *et al.* [CTEQ Collaboration], Eur. Phys. J. C **12** (2000) 375 [arXiv:hep-ph/9903282].
- [32] T. Schafer and E. V. Shuryak, Rev. Mod. Phys. **70** (1998) 323 [arXiv:hep-ph/9610451].
- [33] D. Diakonov and V. Y. Petrov, Nucl. Phys. B **272** (1986) 457.
- [34] D. Diakonov, M. V. Polyakov and C. Weiss, Nucl. Phys. B **461** (1996) 539 [arXiv:hep-ph/9510232].
- [35] K. Goetze, M. M. Musakhanov and M. Siddikov, Phys. Rev. D **76** (2007) 076007 [arXiv:0707.1997 [hep-ph]].
- [36] A. E. Dorokhov, W. Broniowski and E. Ruiz Arriola, Phys. Rev. D **74** (2006) 054023 [arXiv:hep-ph/0607171].
- [37] I. V. Anikin, A. E. Dorokhov and L. Tomio, Phys. Part. Nucl. **31** (2000) 509 [Fiz. Elem. Chast. Atom. Yadra **31** (2000) 1023].
- [38] A. E. Dorokhov and W. Broniowski, Eur. Phys. J. C **32** (2003) 79 [arXiv:hep-ph/0305037].
- [39] H. Kowalski and D. Teaney, Phys. Rev. D **68** (2003) 114005 [arXiv:hep-ph/0304189].
- [40] B. Z. Kopeliovich, I. K. Potashnikova, B. Povh and I. Schmidt, Phys. Rev. D **76**, 094020 (2007), [arXiv:0708.3636 [hep-ph]].
- [41] S. Chekanov *et al.*, (ZEUS Collaboration), PMC Phys. A1, 6 (2007) [arXiv:0708.1478 ].
- [42] F. D. Aaron *et al.* [H1 Collaboration], Phys. Lett. B **659** (2008) 796 [arXiv:0709.4114 [hep-ex]].
- [43] J. Hufner, Yu. P. Ivanov, B. Z. Kopeliovich and A. V. Tarasov, Phys. Rev. D **62** (2000) 094022 [arXiv:hep-ph/0007111].
- [44] B. Z. Kopeliovich, J. Nemchik, A. Schafer and A. V. Tarasov, Phys. Rev. C **65** (2002) 035201 [arXiv:hep-ph/0107227].
- [45] B. Z. Kopeliovich, A. Schafer and A. V. Tarasov, Phys. Rev. D **62** (2000) 054022 [arXiv:hep-ph/9908245].
- [46] E. Iancu, K. Itakura and S. Munier, Phys. Lett. B **590** (2004) 199 [arXiv:hep-ph/0310338].
- [47] H. Kowalski, L. Motyka and G. Watt, Phys. Rev. D **74** (2006) 074016 [arXiv:hep-ph/0606272].
- [48] The exact definition and number of independent GPDs depends on the spin. Below we consider only the simplest case of spin-0 target. Modelling of the helicity components is a much more complicated task which contains large uncertainties.
- [49] The DVCS amplitude in color dipole approach is defined as  $\mathcal{A} \sim \frac{x}{Q^2} \epsilon_\mu^{(i)} \epsilon_\nu^{(j)} \langle p' | J_\mu(z) J_\nu(0) | p \rangle$ , the extra kinematic prefactor  $x^2/Q^4$  is absorbed in the amplitude.